Available online at www.eccomasproceedia.org
Eccomas Proceedia SMART (2023) 426-433

ECCOMAS
Proceedia

X ECCOMAS Thematic Conference on Smart Structures and Materials
SMART 2023
D.A. Saravanos, A. Benjeddou, N. Chrysochoidis and T. Theodosiou (Eds)

ADVANCED NUMERICAL MODELS FOR CAPACITANCE VARIATION OF EMBEDDED PIEZOELECTRIC TRANSDUCERS UNDER MONOTONIC TENSILE TEST

JAMAL NAJD[*,†], ENRICO ZAPPINO[*], ERASMO CARRERA[*], WALID HARIZI[†] AND ZOHEIR ABOURA[†]

[*] Mul2 Group, Department of Mechanical and Aerospace Engineering
Politecnico di Torino
Corso Duca degli Abruzzi, 24 | 10129 Torino, Italy

[†] Université de Technologie de Compiègne, Roberval,
60203 Compiègne Cedex, France

Abstract. For health monitoring applications under static loading, the capacitance variation of embedded polymeric piezoelectric P(VDF-TRFE) transducers was studied. The aim is to compare both experimental and numerical approaches. The experimental results show that the signature of the embedded capacitance follows the strain measurements. On the other hand, the MUL2 FEM tool was used to obtain the change in capacitance numerically while using a higher-order 2D model. A broad parametric study was conducted to investigate the effects of material properties on the results. It was shown that the change, and thus any uncertainty, of material properties (mechanical properties, piezoelectric constants, …) strongly influences the obtained capacitance. With many studies presenting the nonlinear behavior of piezoelectric materials under monotonic tensile loadings, a nonlinear dynamic analysis and further investigation is needed for achieving satisfactory results.

Key words: Smart Structures, Embedded Piezoelectric Materials, Capacitance Variation, Carrera Unified Formulation (CUF).

1 INTRODUCTION

Polymer Matrix Composite (PMC) structures are subjected to different kinds of damage (delamination, fiber breakage, matrix cracking, interfacial debonding...). Such damage is a complex phenomenon that is impossible to predict during the life cycle prior to structural failure. However, due to the convenience of such laminated structures, built up of different laminas, it is possible to embed sensors between the laminas during the manufacturing step, leading to a structure with a sensing capability, i.e. Smart structure. One of the most extensively used sensors in such applications is piezoelectric sensors [1,2]. This is due to their inexpensiveness, versatility and availability. While ceramic piezoelectric transducers (PZTs) offer a good actuation capability, with high mechanical-to-electrical coupling, they are fragile

Peer-review under responsibility of the organizing committee of SMART 2023.
doi: 10.7712/150123.9797.445007

and are easily damaged under high strains. On the other hand, polymeric piezoelectric transducers can be used as sensors thanks to their high ductility allowing them to endure high strains [3].

Under static loading with embedded PZT sensors within PMC material, electric potential variation fails to describe the applied loads due to the occurring dissipation phenomena. Hence, the idea of exploiting the use of other different signatures as Resonance Frequency Measurement, Electrical Impedance Measurement, Decay Time Measurement and Capacitance Measurement [4]. Generally, in our studies, many types of piezoelectric transducers (PZT, PVDF and P(VDF-TRFE)) are used, either embedded or surface mounted. In this study, however, P(VDF-TRFE) was used due to its low thickness and ductility, embedded in the middle of a glass fiber/polyester specimen. Under monotonic tensile mechanical loading, the capacitance variation was studied and it was shown that it follows the shape of the varying load. In order to obtain the results numerically, the MUL2 FEM based on the Carrera Unified Formulation (CUF) was used. With this tool, it is possible to obtain a two-dimensional (2D) model with higher kinematics, allowing the description of to-the-thickness stresses, which have a direct effect on the description of capacitance change in the piezoelectric material. A good correspondence between the numerical and experimental results allows for the connection of the bridge between the two, thus developing a numerical testing benchmark.

2 MATERIAL AND MANUFACTURING

The host composite material made of 22 plies of 2/2 twill glass fabrics each of a surface mass of 280 g/m² and 0.2 mm thickness, infused with a matrix of unsaturated polyester resin **(Norester 822 Infusion, Nord Composites)** and 1% Methyl Ethyl ketone Peroxide hardener**.** The manufacturing process used was the well-known Liquid Resin Infusion (LRI) resulting in a fiber volume fraction v_f = 50%. The embedded round polymeric piezoelectric transducers (D=25mm) of P(VDF-TRFE) 20μm thickness supplied by **Piezotech (Arkema)** were embedded in the middle between the 11th and the 12th layer before the infusion process with average initial capacitance (C_0) of 1.73nF.

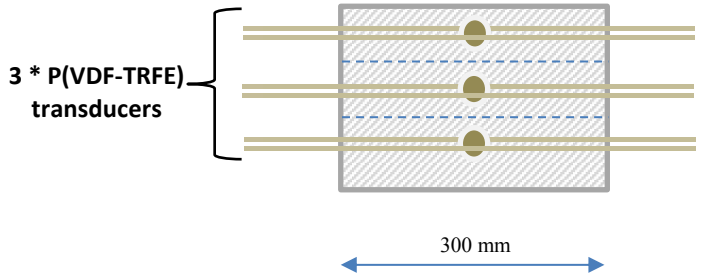

Figure 1: Schema showing the embedding position of P(VDF-TRFE)

The resulting plate was cut into 300*40 mm^2 specimens on which heals were glued at the extremities, using epoxy glue. The schema presented in **Figure 1** shows the plate with the sensors connected and embedded.

3 EXPERIMENTAL TESTING AND RESULTS

The smart specimens were put under monotonic tensile testing with a loading speed of 2 mm/min until failure. During this test, the local strain at the middle of the specimen was measured using an extensometer, and the capacitance measurement was registered using an LRC bridge (**Rohde & Schwarz**, model HM8118, capacitance resolution of 0.01pF).

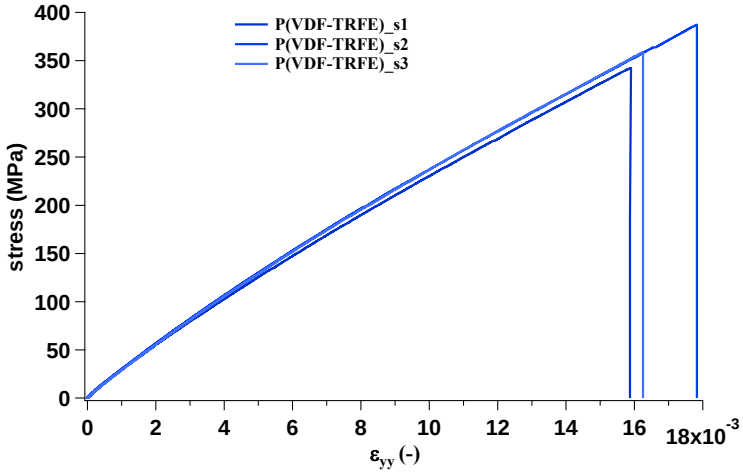

Figure 2: Stress strain curves during the monotonic tensile test of the smart specimens

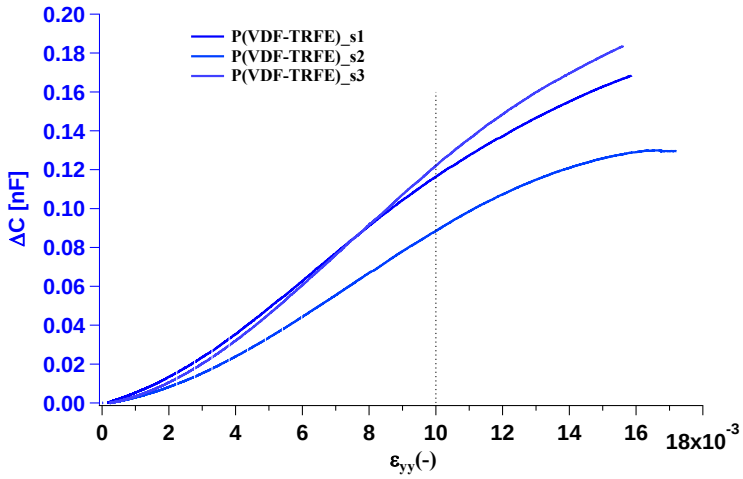

Figure 3: Capacitance change in embedded P(VDF-TRFE) specimens under monotonic tensile test

The results of the capacitance were plotted together with the results extracted from the tensile machine. **Figure 2** shows the stress strain curves obtained in three different smart specimens. The results show the linear behavior of the material up until failure. The strain values reach up to 1.7% before failure with a maximum stress of around 350 MPa. It is also worth mentioning that the specimens exhibit a similar mechanical behavior, where the curves are overlapping.

The capacitance measurement of the three specimens was also plotted as a function of the stresses. The results in **Figure 3** show that the capacitance may exhibit a complex behavior, as even though it follows the stresses applied, the behavior is not the same for the similar transduces, as none of the curves are overlapping.

4 NUMERICAL MODEL

Supposing that the variation of the capacitance exhibits a linear behavior, a 2D model of the static tensile test was proposed, implementing higher kinematics to the thickness of the model. The used numerical model was the in-house MUL2 FEM model based on the CUF. Thanks to this model, it is possible to use the 2D plate model with 3D capacity using higher order model kinematics through-the-thickness. The Lagrange Expansion (LE) kinematics were used as a layer-wise expansion to describe the to-the-thickness unknown vector $q = \{u, v, w, \emptyset\}$ in each layer, where *u, v,* and *w* are the unknowns of the displacement components and $\emptyset$ is the unknown of electric potential. An example of this expansion in linear (B2) element is shown in equation (1):

$$\begin{cases} u = F_1 u_1 + F_2 u_2 \\ v = F_1 v_1 + F_2 v_2 \\ w = F_1 w_1 + F_2 w_2 \\ \emptyset = F_1 \emptyset_1 + F_2 \emptyset_2 \end{cases} \quad (1)$$

where F_1 and F_2 represent the linear Lagrange functions, with (u_1, v_1, w_1, $\emptyset_1$) and (u_2, v_2, w_2, $\emptyset_2$) being are the displacement vectors on the top and bottom nodes of the plate to-the-thickness element respectively. The linear Lagrange functions are expressed in the natural coordinate system of the plate in equation (2):

$$F_1 = \frac{1 + \xi}{2} \qquad F_2 = \frac{1 - \xi}{2} \quad (2)$$

where $-1 < \xi < 1$, with $\xi = -1, 1$ denoting the bottom and top of the plate **Figure 4** and thus, $F_1 = 0, 1$ and $F_2 = 1, 0$ respectively, thus allowing for the continuity of the unknown vector components at the interfaces between two consecutive elements.

Figure 4: Linear Lagrange thickness functions

On the other hand, the strain-charge form of constitutive equations for a coupled piezoelectric problem is given by (3), where σ, ε, D and E represent the stress, strain, electric displacement and electric field vectors respectively, whereas s, d and χ represent the compliance, piezoelectric coefficient and permittivity matrices respectively, with the subscripts E, T indicating that the terms are evaluated at a constant electric field, stress.

$$\varepsilon = s_E \sigma + d^t E \qquad (3)$$
$$D = d\,\sigma + \chi_T\, E$$

As the used piezoelectric material is poled in the z direction, the non-zero electrical displacement component is the z component (D_z) is written as:

$$D_z = d_{31}\sigma_1 + d_{32}\sigma_2 + d_{33}\sigma_3 + \chi_{33}E_3 \qquad (4)$$

The capacitance of a parallel plate capacitor can be described as the charge accumulated on the surface (Q) over the applied voltage (V). This concept in [5] is exploited here, where the surface charge is given by the integral of the electric displacement D_z over the area of the electrode (A).

$$C = \frac{Q}{V} = \frac{\oint_A D_z\, dA}{V} = \frac{\oint_A (d_{31}\sigma_1 + d_{32}\sigma_2 + d_{33}\sigma_3)dA}{V} + \frac{\oint_A \chi_{33}E_3}{V} \qquad (5)$$

The first term of the integral represents the change in capacitance (ΔC) and is the one we are interested in as the second one represents the free capacitor capacitance, $C_0 = \chi_{33}A/d$, where the change in capacitance of 1% in this term due to dimension changes is assumed to be much lower than the experimental capacitance change (~5%) resulting due to the electromechanical coupling.

4.1 Numerical Results

The resulting numerical model can be shown in **Figure 5** (a) where the embedded piezoelectric element was modelled in a circular shape, similar to that of the experimental case. The Layer-wise expansion through the thickness was the cubic (B4) expansion **Figure 5** (b), which allows for the cubic expansion of the unknown vector in each layer.

Table 1: Elastic and piezoelectric properties of the host and embedded piezoelectric materials

Material	E_1	E_2	E_3	ν_{12}	ν_{13}	ν_{23}	G_{12}	G_{13}	G_{23}
GF/Polyester	22.64	22.64	12.11	0.133	0.293	0.293	4.778	4.76	4.76
Unit	GPa	GPa	GPa	-	-	-	GPa	Ga	GPa

Material	E	ν	d_{31}	d_{32}	d_{33}	χ_{33r}
P(VDF-TRFE)	1.0 to 2.6	0.225	6	6	-25 to -28	10
Unit	GPa	-	pC/N	pC/N	pC/N	-

The model was fixed at the surface of one end, and a displacement of 2 mm was imposed on the surface of the heels, leading to a strain ε_{yy} of 1% in the material as the specimen has an effective length of 200 mm between the two heals. The material properties used are listed in **Table 1**, where the piezoelectric material being modelled is the P(VDF-TRFE).

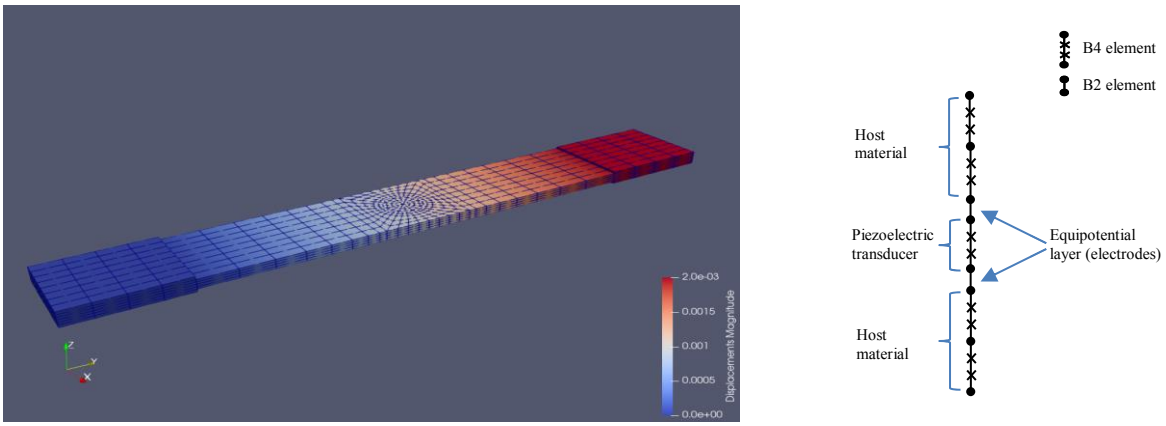

(a) (b)

Figure 5: Showing the numerical tensile test model (a) and the kinematics at the embedding position (b)

As the material properties are not well defined for the piezoelectric material, a parametric study was done where the mechanical and piezoelectric properties were changed to determine the individual effect on the capacitance change. At first, the properties submitted by the manufacturer were used, with E = 1.0 GPa, ν = 0.225, $d_{31} = d_{32}$ = 6 pC/N and d_{33} = -28 pC/N. Other material properties were found in the datasheet of the material, with E= 2.6 GPa, ν = 0.225, $d_{31} = d_{32}$ = 6 pC/N and d_{33} = -25 pC/N. These two instances are referred to as I and II respectively. The modelled capacitance variation for these two instances is ΔC_I = 2.185 nF and ΔC_{II} = 2.21 nF correspondingly, which is significantly higher than that of the experimental results (0.085 nF < ΔC_{exp} < 0.122 nF).

This behavior might be explained by the change of material properties under the embedding process and under the applied stresses. As mentioned in [6,7] for the PZT piezoceramics, the elastic modulus as well as the piezoelectric and dielectric properties of a piezoelectric material change nonlinearly when stresses are applied parallel or perpendicular to the poling direction. As the embedded transducer is subjected to tensile stresses along the tensile test direction and compressive stresses perpendicular to that direction, it is difficult to obtain the exact material properties for the modelling of the embedded transducers as further investigation is needed to assess these parameters (E, d_{13}, d_{33}, χ_{33}) under the conditions and stresses applied during the tensile test. After obtaining these parameters, a non-linear time-dependent modeling approach is necessary, applying the similar approach to acquire the capacitance and its variation.

Due to this difference, a parametric sensitivity study was carried out to determine the effects of the change of the different parameters, the effects of the piezoelectric material stiffness (E), piezoelectric constants (d_{33}, d_{31}), and permittivity effect (χ_{33r}). It can be seen in **Table 2** that the influence of the Elastic modulus (E) is as well as that of the coupling coefficients d_{13}, d_{23} and

d_{33} seem to be almost negligible. The effect of the permittivity χ_{33r} seems to be high. However, one must keep in mind that changing this parameter causes a proportional change in the initial capacitance (C_0) as well, thus, if this parameter decreases, there is a decrease in the initial capacitance, which contributes in the decrease of total capacitance, and vice versa. The summation (ΔC_{tot}) of the two terms ΔC and ΔC_0 is the change in capacitance in this case, which has no major variation with respect to capacitance obtained in the other cases.

Table 2: Sensitivity analysis showing the effect of changing the material property of P(VDF-TRFE) on the capacitance change

General material properties (E = 1.0 GPa, ν = 0.225, $d_{31} = d_{32}$ = 6 pC/N, d_{33} = -28 pC/N and χ_{33r}=10)							
E (GPa)	ΔC (nF)	$d_{31} = d_{32}$ (pC/N)	ΔC (nF)	d_{33} (pC/N)	ΔC (nF)	χ_{33r} (-)	ΔC, ΔC_0, ΔC_{tot} (nF)
0.5	2.168	0	2.433	-30	2.188	2	0.453, 1.738, 2.191
1	2.185	2	2.200	-28	2.185	4	0.886, 1.303, 2.189
1.5	2.197	4	2.189	-26	2.181	6	1.319, 0.869, 2.188
2	2.209	6	2.185	-24	2.178	8	1.752, 0.434, 2.186
2.5	2.220	8	2.184	-22	2.176	10	2.185, 0.000, 2.185
3	2.230	10	2.183	-20	2.173	12	2.619, -0.434, 2.185
3.5	2.240	12	2.184	-18	2.171	14	3.051, -0.869, 2.182

As the numerical results are still far from the numerical ones, further study is needed to understand whether the physical phenomena of capacitance measurement and variation is not well captured in (5) or whether the reason for this discrepancy is due to the material properties. It appears that the effect of the mechanical loading and stresses is overestimated when processing the numerical results, and thus, the capacitance variation obtained is 20 times more than the experimental case. For that, additional preliminary experimental tests and numerical comparison models are needed to well assess the effect of the different parameters involved.

5 CONCLUSIONS

A numerical parametric study regarding the influence of the change in the piezoelectric material properties of P(VDF-TRFE) on the calculated change in capacitance was carried out. The used model was the academic MUL2 FEM tool, using a layer-wise 2D plate model able to evaluate the thickness stresses. In parallel, the experimental results of the capacitance change of the embedded P(VDF-TRFE) under monotonic tensile test were presented, showing the evolution of the capacitance change in both cases. The numerical results obtained overestimate the effect of the applied load on the capacitance variation. As the numerical model used can be relied on, being highly used and well referenced in literature, further study is needed to determine the parameters leading to the inconsistency in the results.

6 ACKNOWLEDGEMENTS

The authors would like to thank the Hauts-de-France Region (France) and Politecnico di Torino (Italy) for the funding of this work as part of the doctoral thesis of Mr. Jamal NAJD (Agreement number 20003877, N GALIS: ALRC2.0-000072).

REFERENCES

[1] C. Tuloup, W. Harizi, Z. Aboura, Y. Meyer, K. Khellil, and R. Lachat, "On the use of in-situ piezoelectric sensors for the manufacturing and structural health monitoring of polymer-matrix composites: A literature review," *Compos. Struct.*, vol. 215, no. December 2018, pp. 127–149, 2019, doi: 10.1016/j.compstruct.2019.02.046.

[2] P. Jiao, K. J. I. Egbe, Y. Xie, A. M. Nazar, and A. H. Alavi, "Piezoelectric sensing techniques in structural health monitoring: A state-of-the-art review," *Sensors (Switzerland)*, vol. 20, no. 13, pp. 1–21, 2020, doi: 10.3390/s20133730.

[3] C. Tuloup, W. Harizi, Z. Aboura, and Y. Meyer, "Integration of piezoelectric transducers (PZT and PVDF) within polymer-matrix composites for Structural Health Monitoring applications: new success and challenges.," *Int. J. Smart Nano Mater.*, no. September, 2020, doi: 10.1080/19475411.2020.1830196.

[4] K. Kim, J. Kim, X. Jiang, and T. Kim, "Static Force Measurement Using Piezoelectric Sensors," *J. Sensors*, vol. 2021, 2021, doi: 10.1155/2021/6664200.

[5] J. Najd, E. Zappino, E. Carrera, W. Harizi, and Z. Aboura, "A variable kinematic model for the prediction of capacitance variations in embedded PZT sensors," *J. Intell. Mater. Syst. Struct.*, vol. 34, no. 7, pp. 811–824, 2023, doi: 10.1177/1045389X221121974.

[6] G. Yang, S. Liu, W. Ren, and B. K. Mukherjee, "Effects of uniaxial stress on the piezoelectric, dielectric, and mechanical properties of lead zirconate titanate piezoceramics," *Ferroelectrics*, vol. 262, pp. 207–212, 2001, doi: 10.1080/00150190108225151.

[7] S. W. MAHON, D. MOLONEY, F. LOWRIE, and A. R. BOWLES, "Stress dependence of the piezoelectric, dielectric and elastic properies of PZT ceramics," in *Proceedings of the NATO Advanced Research Workshop on Piezoelectric Materials: Advances in Science, Technology and Applications*, 1999, pp. 159–168.